Dendrobranchiata Chitin Deacetylation Degree and its Potency as Iron (III) Ion Adsorbent from Aqueous Solution

Oluwashina Philips Gbenebor[*]*, Abimbola Patricia Idowu Popoola*

Department of Chemical, Metallurgical and Materials Engineering, Tshwane University of Technology, Pretoria, South Africa

✉: philipsogbenebor@gmail.com, iD: *0000-0003-1693-4601*, 0000-0003-4447-8551*

Abstract

This research investigates the production of epoxy resin composites reinforced by the synthesized heavy tungsten alloys (W-7Zn-3Co-Y₂O₃). Y₂O₃ is used for dispersion of the compound during the ball milling process. Laminating resin component A and hardened component B were used to produce polymer epoxy matrix. The tungsten heavy alloys reinforced epoxy composites were examined in terms of Vickers hardness, density measurement and microstructural characterization . The results indicate that the 16 hour-milled reinforced epoxy composites have the highest hardness value.

Keywords: Tungsten alloys, mechanical alloying, and polymer epoxy composites

1. Introduction

The quest to improve man's standard of living has engendered further creation and developments of industries which in turn, has hastened urbanization growth. Discharge of domestic wastes including those from industries' processing operations such as chemicals into water has made it harmful for human use Organic pollutants have been found to be biodegraded by microbes to products useful to marine life [1]. Heavy metals such as lead (Pb), Nickel (Ni), copper (Cu), chromium (Cr), zinc (Zn), cadmium (Cd), arsenic (As), and iron (Fe), are harmful because of their non-biodegradable nature [2-3]. They mostly emanate in high concentrations from industries including mining, metal ore processing and electroplating industries as effluents [4]. Heavy metals have also been reported to gain access to the environment via soil erosion, rock weathering and pesticides applied to crops [5]. Waste water irrigation has been reported by Muchuweti et al. [6] to contaminate the soil which ends up poisoning the foods obtained from the plants that grow on the contaminated soil. Animals graze on these poisoned plants, drink from the polluted waters and thus have the heavy metals accumulated in their tissues. Marine lives breeding in the heavy metal-polluted water are not left out; all living things within a given ecosystem are contaminated along their cycles of food chain. Over the years, various techniques including precipitation, adsorption, oxidation, coagulation, flocculation and membrane filtration processes have been devised to eliminate these heavy metals from waste waters. Adsorption has been considered to be an economical technique as it offers the use of low cost adsorbents effective in treatment of water. In recent years, use of biopolymers as bio adsorbents has gained wide recognitions owing to their biodegradability, non-toxicity, accessibility and low cost of procurement. Among natural polymers, polysaccharide such as chitin has been confirmed an effective absorbent. Second to cellulose in terms of natural polymer abundance, chitin is a linear polysaccharide of $(1 \rightarrow 4)$ linked units of *N* -acetyl-2- amino-2-deoxy- D – glucose [7]. While hydroxyl (OH) group exists on carbon C2 in cellulose, acetamide (RCONH₂) group is formed on C2 in chitin; this gives a major structural difference between the two polysaccharides. The appreciable biodegradability and biocompatibility of chitin are responsible for its applications in

wound dressings where sponges [8] and suture threads [9] are being used. Its high thermal stability [10] enhances its suitability as a food packaging material. The degree of chitin acetylation (DA) is the percentage of acetyl (RC=O) groups present in chitin. Nam et al. [11] explains it as the ratio of *N*-acetylated group to *N*-de acetylated (amino, RNH$_2$) groups. This parameter is often used to identify chitin and its derivative – chitosan. According to Kim, [12], a biopolymer is chitin when DA > 50 % while that lower than this value is classified as chitosan. Chitin has been used in the adsorption of Ar, Zn, Cu, Cd, Mn, Fe, Pb and Cr [13-17]. Jaafarzadeh et al. [13] synthesized chitin from shrimp shells by using 10% v/v hydrochloric acid (HCl) and sodium hydroxide (NaOH) as demineralization and deproteinization reagents respectively to adsorb Zn^{2+} from aqueous solutions. Ease of Zn^{2+} removal was ascribed to the increase in pH and chitin dose. Pulverized Bargi fish scales have been treated with 5% v/v HCl to remove calcium carbonate, CaCO$_3$ [18]. Chitin produced was used in removing Cr^{6+} from aqueous solutions of potassium dichromate (K$_2$Cr$_2$O$_7$) salt. The researchers concluded that the adsorption process was temperature and pH dependent as maximum adsorption capacity was attained at pH 6-8. In the works conducted by Forutan et al. [17], shells of pink shrimps were refluxed 7%v/v HCl and NaOH to extract chitin that would be suitable for the adsorption of Pb from lead stock solutions. Optimum conditions of pH, contact time, bioadsorption dosage and initial concentration of Pb were observed to be 9, 200 min, 5gr/L and 7.99ppm respectively. The best efficiency biosorption was discovered to be 99.7%. Chitosan has been processed from chitin sourced from crab shell for the removal of heavy metals from contaminated water [16]. Mineral such as CaCO$_3$ was eliminated from the crushed crab shells using 10% v/v HCl followed by protein removal with NaOH using the same concentration between 103-105 °C. zinc chloride (ZnCl$_2$), Nickel chloride (NiCl$_2$), iron (III) chloride (FeCl$_3$), lead chloride (PbCl$_2$), cadmium chloride (CdCl$_2$), manganese (II) sulphate (MnSO$_4$) and chromium (III) sulphate (Cr$_2$(SO$_4$)$_3$) were used for chemical solutions. Chitosan was found to remove metal in the order Mn>Cd>Zn>Co>Ni>Fe>Pb>Cr. Concentrations of 2N HCl and 1N NaOH (at 80 °C) were used by Bhavani et al. [19] to process chitin from crab shells. Chitin produced was deacetylated by further reactions with 40% v/v NaOH at 110 °C for chitosan synthesis. The biopolymer served as a potential adsorbent of Cu^{2+}, Zn^{2+}, Cr^{6+}, Cd^{2+} and Pb^{2+} from electroplating water waste. Results gathered from existing researches have shown that removal performance of chitin bioadsorbents is not similar for all heavy metals. This could be attributed to the different experimental techniques and conditions considered. This justifies the submissions of Bhavanio et al. [19] who affirmed that high reactivity and selectivity of chitin towards compounds and metals are due to the presence of chemical reactive OH, RCONH$_2$ or RNH$_2$ groups in their polymer chains. The functionalities of these groups in chitin have been confirmed to be dependent on their source of origin as identified from previous works [20-22]. In this study, chitin isolated from prawn exoskeleton possessing different deacetylation degree (DDA) is characterized for its thermal and structural properties. In addition, the influence of chitin's varying DDA on its potency for Fe adsorption is investigated. Excess Fe in the body has been reported to cause osteoporosis as it prevents the differentiation and proliferation of osteoblasts [23]. Abnormal hepatic gluconeogenesis is another effect of Fe overload in the human body [24].

2. Materials and Methods

2.1. Chitin extraction

Exoskeletons of prawns were washed, dried and ground to 200 μm particle sizes. Demineralization was carried out by treating ground particles with 1M HCl until no evidence of CO$_2$ release was noticed. The demineralized samples were washed with distilled water to neutral pH, filtered and oven dried at 70 °C till it was completely dry. The demineralized powders were refluxed with 1 M NaOH at 100 °C for 1, 2, 3, 4 and 5 h to complete the deproteinization process.

Samples were washed, filtered and dried as earlier done for demineralized powders and chitin was finally obtained. In this study, C1, C2, C3, C4 and C5 designations are used to identify chitin extracted by deproteinizing for 1, 2, 3, 4 and 5 h respectively

2.2. Chitin characterizations

2.2.1. Fourier Transform Infrared Spectroscopy (FTIR)

Functional groups present in each chitin sample were identified using Nicolet 6700M spectrometer and processed at a resolution of 4 cm^{-1}. Spectra were taken in the absorbance mode between 500–4000 cm^{-1}. The degree of deacetylation, DDA was calculated using the formula in Eq. (1):

$$DDA\ (\%) = 100 - DA \tag{1}$$

Where DA is the degree of chitin acetylation which was calculated using Eq. (2): [20, 26]:

$$DA = \frac{A_{1650}}{A_{3450}}\ x\ \frac{100}{1.33} \tag{2}$$

Amide I absorbance variation is represented by A_{1650}; OH absorbance variation is represented by A_{3450}; for full N-acetylated chitin ratio A_{1650}/A_{3450} is represented by the factor 1.33.

2.2.2. Thermogravimetric analysis (TGA)

Two milligram of each chitin sample was heated to 750 ºC using TGA Q500 device at10 ºC/min heating rate. From the thermograms, temperatures at the commencement and conclusion of chitin decomposition were quantified.

2.2.3. X-Ray diffraction

A monochromatic Cu Kα radiation from a PANanalytical device operated at 40 kV and 40 mA, was targeted at each chitin sample. The crystallinity, Crl was calculated from the diffractogram using Eq. (3) [27]:

$$Crl\ (\%) = [I_c\ /(I_c + Ia)]\ x\ 100 \tag{3}$$

Where I_a and I_c are intensities of crystalline and amorphous peaks respectively
Crystalline size of chitin samples were calculated using Eq. (4) [28]:

$$D_{hkl} = k\lambda /\ \beta cos\ \theta \tag{4}$$

Value of K is assumed to maintain a constant value of 1.It stands for perfection of crystallite; incident radiation wave length (1.5406) is represented byλ; β (rad) represents the width of the crystalline peak at half height; and θ (deg) stands for diffraction angle that corresponds to the crystalline peak.

2.2.4. Scanning Electron Microscopy (SEM)

Samples were coated win Au to enhance proper electrical conductivity which was scanned using an ASPEX 3020 model variable pressure SEM to identify the morphological features of chitin particles.

2.3. Preparation of Fe³⁺ - rich solution and determination of chitin sorption capacity

A gram of iron (III) chloride ($FeCl_3$) was dissolved in 1 L distilled water at room temperature. In this study, effects of pH (which ranged from 1-6) and contact time on Fe^{3+} adsorption capacity of chitin samples were investigated. Chitin particles (0.5 g) was added to 100 ml $FeCl_3$ solution and continuously stirred at room temperature for 30, 60, 90, 120, 150 and 180 min, which were the contact times. To calculate the sorption capacity (q) of chitin, Eq. (5) [29] was used:

$$q \text{ (mg/g)} = [(C_o - C_i)/W]\ V \tag{5}$$

The initial and final concentrations of Fe^{3+} in the solution is represented by C_o and C_i (mg/L) respectively; W represents the mass of chitin (g) and V stands for the volume of aqueous solution (L). As regards adsorption tests, chitin samples with the highest and lowest DDA were selected. An additional sample whose DDA value lied between these two was also chosen to make the total samples characterized for the adsorption tests three.

3. Results and Discussions

3.1. Functional groups and DDA

The FTIR spectra of C1, C2, C3, C4 and C5 are shown in Fig.1. Apart from different intensities displayed, pattern of all chitin samples are similar. Their existing functional groups are given in Table 1.
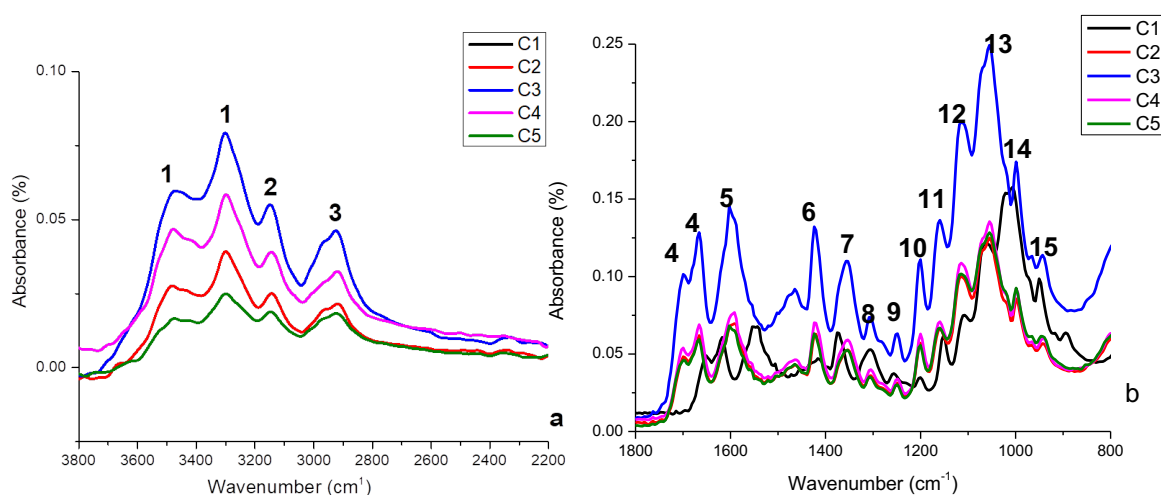

Fig. 1. FTIR spectra of chitin between (a) 3800 – 2200 cm⁻¹ and (b) 1600 – 800 cm⁻¹

Maximum DDA (43.8 %) is obtained when chitin was deproteinized for 5 h (Fig.2) and this shows that gradual increase in reaction time between demineralized prawn exoskeleton and NaOH steadily removes *N*-acetyl groups in the glucopyranose units of the final product (chitin). This simultaneously raises the number of RNH_2 in the polymer chain. Result obtained from this study shows that sufficient reaction time during deproteinization engenders the instability of the bond in $RCONH_2$. Also, this result informs that NaOH concentration alone will not influence DDA as earlier demonstrated in the investigation of Gbenebor et al. [20]. Aranaz et al. [30] reported that there is usually a reduction in the resistance of $RCONH_2$ on the C2-C3 substituent arrangement of the glucopyranose chitin ring. This could have triggered hydrolysis of the group ($RCONH_2$) by virtue of increasing deproteinization time.

Table 1. Functional groups of prawn chitin

| S/N	Functional groups	Wavenumber (cm^{-1})
1	OH stretching	3443-3487; 3259-3298
2	NH stretching	3096-3149
3	Symmetric Ch$_3$ stretching and asymetric CH$_2$ stretching	2925
4	C=O secondary amide stretch (Amide I)	1661, 1626
5	NH bend, CN stretch (Amide II)	1559
6	CH2 bending and CH$_3$ deformation	1416
7	CH bending and Ch$_3$ symmetric deformation	1379
8	CH$_2$ wagging (Amide III)	1312
9	Asymmetric bridge oxygen stretching	1157
10	Asymmetric in -phase ring stretching mode	1117
11	C-O-C asymetric stretch in phase ring	1074
12	CO stretching	1028
13	CH$_3$ wagging along chain	933
14	CH stretching (saccharide rings)	897
15	NH out-plane bending	750
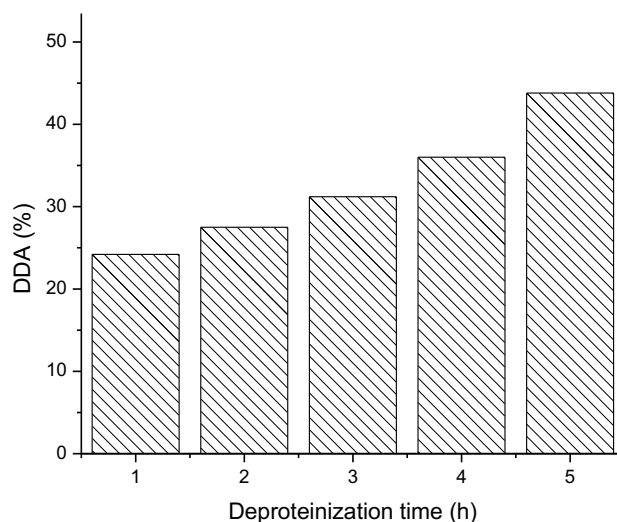
Fig. 2. DDA of chitin as a function of deproteinization time

3.2. Thermal response and chitin content

There exist two stages of decomposition (Fig. 3) – the first, which is a minor step, occurs between 50 – 110 °C and this represents the evaporation of moisture content in chitin. The second decomposition stage is a major step which commences between 161 and 309 °C (T$_{onset}$) and ends (T$_{finish}$) between 260 and 438 °C. This major decomposition represents the existence of chitin, which is similar to the findings of Gbenebor et al. [20]. One of or the combination of denaturation, depolymerization and degradation according to Juarez de la Rosa et al. [31] exist(s) within this temperature range. Here, chitin's structure becomes devoid of CH$_3$-CH$_2$ in aliphatic compounds;

decompositions of C=O and NH in Amides I and II proceeds after and finally, C-O-C in the saccharide separates from chitin. [27].The values of T_{onset}, T_{finish}, contents of moisture, chitin and residue are displayed in Table 2. In this study, thermal stability is defined as the minimum temperature at which chitin molecular bonds begin to disintegrate (this is determined by comparing magnitudes of T_{onset}). It is noticed in this study that thermal stability of chitin sample reduces with increase in deproteinization time as the maximum T_{onset} is recorded at 309 ºC for C1 while C5 maintains the least T_{onset} at 161 ºC. Presence of the most thermally stable *N*-acetyl (GlcNAc) units in C1 could be responsible for this. Kahdestani et al. [32] characterized chitosan for TGA and observed its T_{onset} to attain a magnitude of 195 ºC while Nam et al. [11] reported chitosan samples to exhibit T_{onset} values between 164 and 174 ºC. This shows that C5 will possess features close to chitosan. It can also be confirmed from this study that residue and chitin contents may not be dependent on deproteinization time.
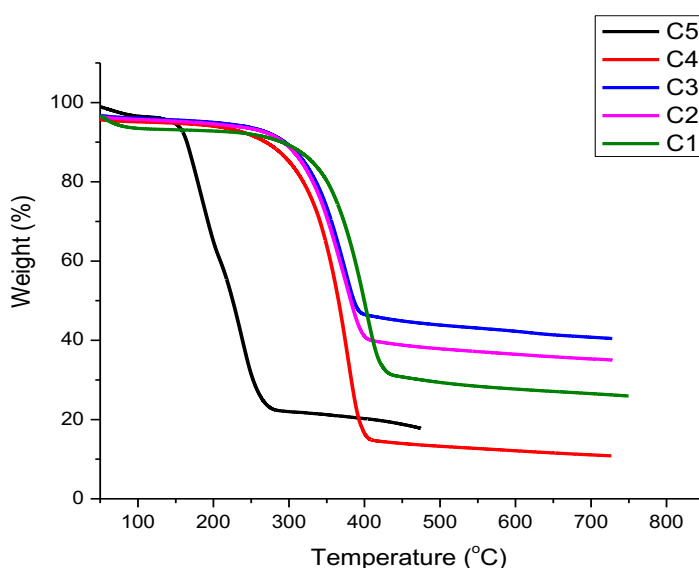

Fig. 3. TGA of isolated chitin after 1, 2, 3, 4 and 5 h deproteinization

Table 2. TGA parameters of isolated chitin after 1, 2, 3, 4 and 5 h deproteinization

S/N	Chitin	T_{onset} (^{0}C)	T_{finish} (^{0}C)	Chi mass loss (%)	Moisture (%)	Residue (%)
1	C1	309	438	61.1	8.9	30.0
2	C2	294	401	57.0	7.0	36.0
3	C3	284	391	48.7	6.3	45.0
4	C4	278	405	77.0	8.4	14.6
5	C5	161	260	72.7	5.2	22.1

3.3. Crystalline properties

X-ray diffraction of chitin samples are shown in Fig. 4. All samples follow similar patterns but with different intensities, indicating the effect of prolonged NaOH reactions. A major peak (19.5º) corresponds to (110) while other four peaks of 9.8, 20.6, 23.4 and 26.5^0 diffracting on (020), (120), (130) and (013) are observed. Increasing deproteinization time culminates in reduction in peak intensities of each sample. The Crl of C1 is 84.5% while 81.3, 78.3, 73.8 and 67.8% are calculated for C2, C3, C4 and C5 respectively. This implies that the structural stability

of chain decreases as a result of gradual removal of *N*-acetyl groups, which eventually scales down its crystallinity. The crystallite sizes (D_{hkl}) of chitin samples processed from varying deproteinization times are illustrated in Table 3 Information from the results imply that the lower the average crystallite size, the less crystalline the polysaccharide. The lowest Crl processed by C5 could be responsible for its least response to thermal energy as discussed in Fig. 3.
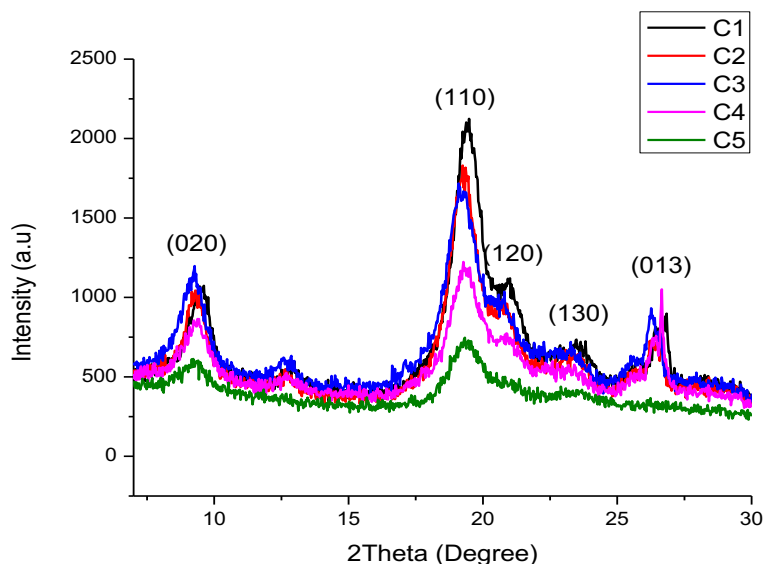

Fig. 4. XRD of isolated chitin after 1, 2, 3, 4 and 5 h deproteinization

Table 3.Crystallite properties and crystallinity of isolated chitin after 1, 2, 3, 4 and 5 h deproteinization

S/N	Chitin	D_{020} (Å)	D_{110} (Å)	D_{120} (Å)	D_{130} (Å)	D_{130} (Å)	Average (Å)	Crl (%)
1	C1	0.6004	1.1821	0.1792	83.874	0.0386	17.170	84.5
2	C2	1.3823	1.2483	1.5558	0.6918	1.3988	1.2554	81.3
3	C3	0.9757	1.3594	0.4997	0.2748	2.6899	1.1599	78.3
4	C4	0.7438	1.816	0.4973	0.0348	0.2864	0.6767	73.8
5	C5	0.4285	0.943	--	0.0505	--	0.4707	67.8

3.4. Morphology

The morphology of C1 as presented in Fig. 5a shows a plate-like fibrillar form. This fibrillar nature is also processed by C2, but with a reduced geometry (Fig. 5b). It is noticed in this study that prolonged deproteinization time makes the surface of chitin particles look shiny/bleached. This could be an indication of gradual reduction of nitrogen and carbon in C=O and CN (from Amides I and II). There has been steady reduction in size of these plate-like fibrils as deproteinization time was carried out for 3, 4 and 5 h (Fig. 5c-e).
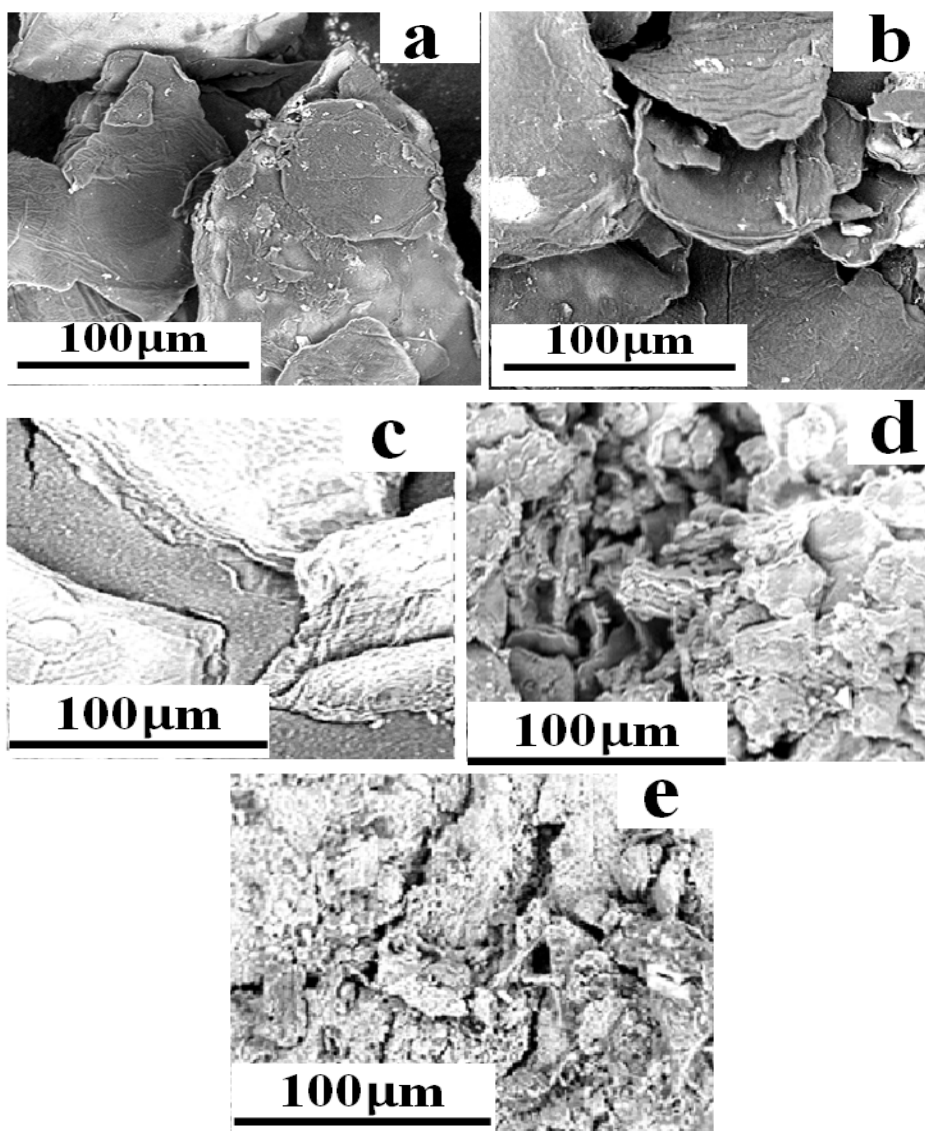
Fig. 5. SEM of chitin (a) C1 (b) C2 (c) C3 (d) C4 (e) C5

3.5. Effect of contact time on Fe^{3+} sorption capacity of chitin

The concentration of Fe^{3+} that can be adsorbed on to chitin samples (C1, C3 and C5) by virtue of chitin - Fe^{3+} contact time between 30 – 180 min was investigated at room temperature, pH 5 and 150 rpm stirring speed. It is evident from Fig. 6 that for each chitin, the amount of Fe^{3+} adsorbed increases from 30 min and reaches a maximum value at 120 min. Within these periods, it can be reported that chitin provides favourable surface areas for Fe^{3+} adsorption. Beyond 120 min contact time, adsorption capacities of each chitin sample gradually drop and this can be attributed to saturation of surfaces occupied by Fe^{3+}. This is similar to the investigation of Gokila et al. [33] who confirmed that the decline in adsorption capacity of chitosan-alginate-nanocomposite on Cr^{6+} after 300 min was ascribed to the exhaustion of adsorption sites as there were no more unsaturated surfaces for adsorption. Chitosan has been used as adsorbent on Pb and Ni [34], After 180 min, the amount of Pb^{2+} and Ni^{2+} remained constant. The maximum content of NH_2 groups as depicted by the highest DDA (43.8 %) may be responsible for the best adsorption performance displayed by C5. Its ability to allow aqueous solutions penetrate through its structure owing to its least value of Crl (67.8 %) may also be a determining factor for its best adsorption display. The Crl and DDA of C3 are 78.3 % and 31.5 % respectively; this implies there exists 31.5 % of NH_2 groups compared to C1 that has 24.2 %. It (C3) will still give room

for aqueous solution penetration into its structure than C1 whose Crl is 84.5 %. This could be the reason why the Fe^{3+} adsorption feature of C3 > C1.
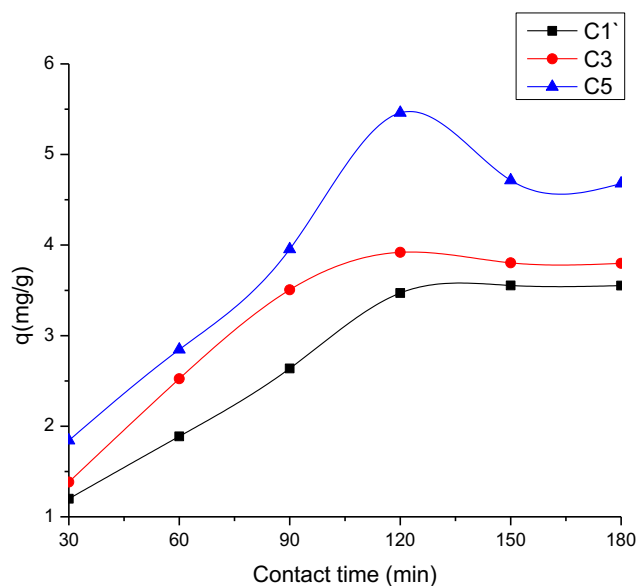

Fig. 6. Effect of contact time on Fe^{3+} adsorption capacity of C1, C3 and C5

3.6. Effect on pH on Fe^{3+} sorption capacity of chitin

Fig. 7 shows the effect of pH on the adsorption of Fe^{3+} by chitin samples (C1, C3 and C5). Results were taken for pH values ranging between 1 and 6 at constant stirring speed (150 rpm) and contact time of 120 min at room temperature. The pH has been confirmed to an important parameter that influences ionization degree of metal, solubility of metal ions and surface features of adsorbent [19, 35]. Each sample display improved Fe^{3+} adsorption performance as the pH gradually increases to a maximum sorption coefficient at pH 5. At lower pH, the solution is acidic and there will be electrostatic repulsion between H^+ and Fe^{3+} which compete for bonding sites on chitin surface. In addition, NH_2 groups in chitin are protonated by the high concentrations of H^+ in the acidic solution; this further engenders repulsion of Fe^{3+}. As the pH values increase, the concentration of H+ in the solution decreases as well as NH_2 protonation. This elevates the sorption coefficient of each chitin sample as more binding surface is increased and electrostatic repulsion is limited [36-37]. Although all chitin samples display adsorption potency for Fe^{3+}, C5 shows the best performance and this can be attributed to the highest DDA it possesses. It implies that the sample (C5) has the highest density of free NH_2 groups that culminates in creation of active adsorption sites. This is a feature that makes chitosan a better heavy metal adsorbent than chitin [38]. Beyond pH5, adsorption capacities of C1, C3 and C5 drop as a result of a likelihood of a metal hydroxide ($Fe(OH)_3$ in this case) formed which could have prevented the metal ions from contacting chitin active site [39].
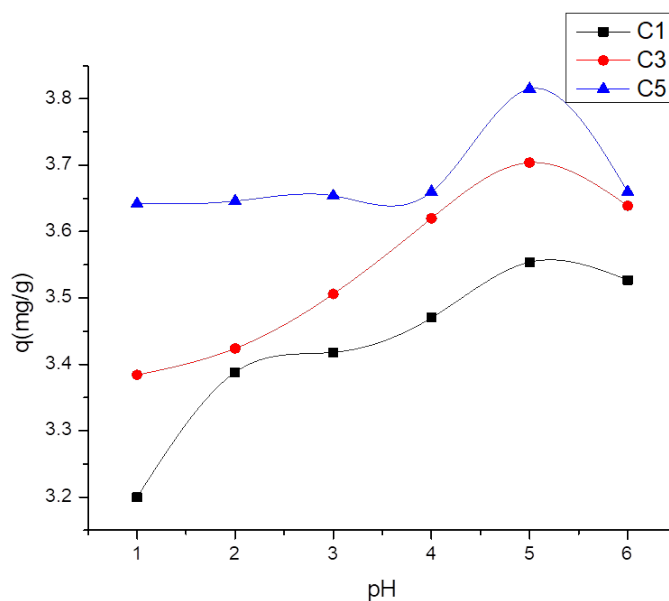
Fig.7. Effect of pH on Fe^{3+} adsorption capacity of C1, C3 and C5

4. Conclusions

Influence of deproteinization time on the properties of prawn chitin has been successfully studied. Thermal stability of chitin decreases as the time allowed for deproteinization increases. More time is allowed for the glycosidic bonds in chitin to disintegrate and on the 5th hour, the thermal characteristics of the sample is comparable to that of chitosan as this is justified by its lowest DDA value of 43.8 %. There is also a gradual decrease in chitin's crystallinity from 84.5 to 67.8 % after deproteinization from 1 to 5 h. This implies that the bond strength in chitin can be altered as more of RNH_2 groups are formed during deacetylation. Results from this study have shown that RC=O groups are responsible for chitin strength and will thus play important role in its thermal and structural properties. Sorption capacity of selected chitin for Fe^{3+} offers its best performance at pH 5 and 120 min contact time at room temperature and constant stirring sped (150 rpm). It can be affirmed that existence of more RNH_2 in chitin improves the adsorption potency of chitin and that is why in terms of Fe^{3+} adsorption performance, C5 (DDA 43.8 %) > C3 (DDA 31.5 %) > C1 (DDA 24.2 %). This study has been able to establish that apart from reagent type, temperature and concentration considered during deproteinization, reaction time is also a notable parameter that can affect the structure and performance of chitin. Further studies are ongoing with the aim of considering the kinetics and mechanisms involved in the interactions between chitin adsorbents (of different physical and structural modifications) and other heavy metals including Fe.

References

[1]   Sankhla, M.S., Kumari, M., Nandan, M., Kumar, R. and Agrawal, P., Heavy Metals Contamination in Water and their Hazardous Effect on Human Health- A Review. *International Journal of Current Microbiology and Applied Sciences*, 5(10), 759-766, 2016.

[2]   Verma, R. and Dwivedi, P., Heavy Metal Water Pollution- A Case Study. *Recent Research in Science and Technology*, 5(5), 98-99, 2013.

[3]   Jaishankar, M., Tseten, T., Anbalagan, N., Mathew, B.B. and Beeregowda, K.N.,Toxicity, Mechanism and Health Effects of Some Heavy Metals. *Interdisciplinary Toxicology,* *7*(20), 60-72, 2014.

[4]   Anastopoulos, I., Bhatnagar, A., Bikiaris, D.N. and Kyzas, G.Z., Chitin Adsorbents for Toxic metals: A Review. *International Journal of Material Sciences*, 18(114), 1-111, 2017.

[5]   Morais S, Costa F.G, and Pereira, M.L., Heavy Metals and Human Health, Environmental health – emerging issues and practice, Chapter 10, 227–246, 2012.

[6]   Muchuweti, M., Birketi, J.W., Chinyanga, E., Zvauya, R., Scrimshaw, M.D. and Lester, J.N., Heavy Metal Contents of Vegetables Irrigated with Mixture of Wastewater and Sewage Sludge in Zimbabwe: Implications for Human Health. *Agriculture, Ecosystems & Environment,* 112, 41-48, 2006.

[7]   Zhao, Y., Ju, W.T., Jo, G.H., Jung, W.J. and Park, R.D., Perspectives of Chitin Deacetylase Research. *Biothechnology of Polymers*, 131-144, 2011.

[8]   Li, S., Li, X., Zheng, L., Ruiz-Hitzky, E., Xu, . and Wang, X., MXene-Enhanced Chitin Composite Sponges with Antibacterial and Hemostatic Activity for Wound Healing. *Advanced Health Care Materials*, 1-6, 2022.

[9]   Odili, C.C., Ilomuanya, M.O., Sekunowo, O.I., Gbenebor, O.P. and Adeosun, S.O., Knot Strength and Antimicrobial Evaluations of Partially *Absorbable Suture. Progress in Biomaterials*, 12, 51–59, 2023.

[10]   Gbenebor, O.P., Adeosun, S.O., Adegbite, A.A. and Akinwande A., Organic and Mineral Acid Demineralizations:Effects on *Crangon* and *Liocarcinus Vernalis* –Sourced Biopolymer Yield and Properties. *Journal of Taibah University for Science*, 1*2*(6), 837-845, 2018.

[11]   Nam, Y.S., Park, W.H., Ihm, D. and Hudson, S.M., Effect of the Degree of Deacetylation on the Thermal Decomposition of Chitin and Chitosan Nanofibers. *Carbohydrate Polymers.* 80, 291-295, 2011.

[12]   Kim, S., Chitin, Chitosan, Oligosaccharides and their Derivatives; Biological and their Bpplications. *CRC Press*, *Taylor & Francis Group*, 3-633, 2011.

[13]   Jaafarzadeh, N., Mengelizadeh, N., Takdastan, A., Heidari-Farsani, M. and Niknam, N., Adsorption of Zn(II) from Aqueous Solution by using Chitin Extraction from Crustaceous Shell. *Journal of Advances in Environmental Health Research*, *2*, 110–119, 2014.

[14]   Jaafarzadeh, N., Mengelizadeh, N., Takdastan, A., Farsani, M.H., Niknam, N., Aalipour, M., Hadei, M. and Bahrami, P., Biosorption of Heavy Metals from Aqueous Solutions onto Chitin. International Journal of Environmental Health Engineering, 4, 1–7, 2015.

[15]   Kocer, N.N., Uslu, G. and Cuci, Y., The adsorption of Zn(II) Ions onto Chitin: Determination of Equilibrium, Kinetic and Thermodynamic Parameters. *Adsorption Science &* Technology, *2* (26), 333–344, 2008.

[16]   Rana, M.M., Removal of Heavy Metal from Contaminated Water by Biopolymer Crab Chitosan. *Journal of Applied Sciences*, 9(15), 2762 - 2769, 2009.

[17] Forutan, R., Ehsandoost, E., Hadipour, S., Mobaraki, Z., Saleki, M. and Mohebbi3, G., Kinetic and Equilibrium Studies on the Adsorption of Lead by the Chitin of Pink Shrimp (Solenocera melantho). *Entomology and Applied Science*, 33(3), 20-26, 2016.

[18] Otuonye, U.C., Barminas, J.T., Magomya1, A.M., Kamba, E.A. and Andrew, C., Removal of Chromium (VI) as a Heavy Metal from Aqueous Solution using Chitin Obtained from Bargi Fish (Heterotis Miloticus) scale. *Sci-Afric Journal of Scientific Issues, Research and Essays*, 2 (3), 128-131, 2014.

[19] Bhavani, K., Roshan, B.E., Selvakumar, S. and Shenbagarathai, R., Chitosan– A low Cost Adsorbent for Electroplating Waste Water Treatment. *Journal of Bioremediation & Biodegradation*, 7(3), 1-6, 2016.

[20] Gbenebor, O.P., Adeosun, S.O., Lawal, G.I., Jun, S. and Olaleye, S.A., Acetylation, Crystalline and Morphological Properties of Structural Polysaccharide from Shrimp Exoskeleton. *Engineering Science and Technology, an International Journal*, 20, 1155–1165, 2017a.

[21] Gbenebor, O.P., Akpan, E.I. and Adeosun, S.O., Thermal, Structural and Acetylation Behavior of Snail and Periwinkle Shells Chitin. *Progress in Biomaterials*, 6, 97–111, 2017b.

[22] Akpan, E.I., Gbenebor, O.P. and Adeosun, S.O., Synthesis and Characterization of Chitin from Periwinkle (Tympanotonus Fusatus (L.)) and Snail (Lissachatina Fulica (Bowdich)) Shells. *International Journal of Biological Macromolecules*, **106**, 1080-1088, 2018.

[23] Yamasaki, K. and Hagiwara, H., *Excess Iron Inhibits Osteoblast Metabolism. Toxicology Letters*, 191(2-3), 211-215, 2009.

[24] Lee, H.J., Choi, J.S., Lee, H.J., Kim, W.H., Park, S.L. and Song, J., Effects of Excess Iron on Oxidative Stress and Gluconegenesis through Hepcidin During Mitochondrial Dysfunction. *The Journal of Nutritional Biochemistry*, 26(12), 414-1423, 2015.

[25] Lee, H.J., Choi, J.S., Lee, H.J., Kim, W.H., Park, S.L. and Song, J., Effects of Excess Iron on Oxidative Stress and Gluconegenesis through Hepcidin During Mitochondrial Dysfunction. *The Journal of Nutritional Biochemistry*, 26(12), 414-1423, 2015.

[26] Kaya, M., Seyyar, O., Baran, T. and Turkes, T., Bat Guano as New and Attractive Chitin and Chitosan Source.. *Frontiers in Zoology*. 11, 1-1-10, 2014.

[27] Juarez-de la Rosa, B.A., Quintana, P., Ardisson, P.L., Ya´nez-Limon, J.M. and Alvarado-Gil, JJ., Effects of Thermal Treatments on the Structure of Two Black Coral Species Chitinous Exoskeleton. *Journal of Materials Science*, 47, 990–998, 2012.

[28] Al-Sagheer, F.A., Al-Sughayer, M.A., Muslim, S. and Elsabee, M.Z., Extraction and Characterization of Chitin and Chitosan from Marine Sources in Arabian Gulf. *Carbohydrate Polymers*, 77, 410–419, 2009.

[29] Jaafarzadeh, N., Mengelizadeh, N. and Hormozinejad, M., Adsorption of Zn (II) Ion from Aqueous Solution by using Chitin Extracted from Shrimp Shells. Jentashapir *Journal of Health Research,* 5(3), 133 – 138, 2014.

[30] Aranaz, I. , Mengíbar, M., Harris, R., Paños, I. Miralles, B., Acosta, N., Galed, G. and Heras, A., Functional Characterization of Chitin and Chitosan. *Current Chemical Biology.* 3, 203–230, 2009.

[31] Juárez-de la Rosa, B.A., Crespo, J.M., Owen, Q., Gónzalez-Gómez, W.S.,Yañez-Limón, J.M., and Alvarado-Gil, J.J., Thermal Analysis and Structural Characterization of Chitinous Exoskeleton from Two Marine Invertebrates. *Thermochimica Acta.* 610, 16–22, 2015.

[32] Kahdestani, S.A., Shahriari, M.H. and Abdouss, M., Synthesis and Characterization of Chitosan Nanoparticles Containing Teicoplanin using Sol–Gel. *Polymer Bulletin*, 78, 1133–1148, 2021.

[33] Gokila, S., Gomathi, T., Sudha, P.N. and Anil, S., Removal of the Heavy Metal ion Chromiuim(VI) using Chitosan and Alginate Nanocomposites., *International Journal of Biological Macromolecules,* 104, 1459-1468, 2017.

[34] Akinyeye, O.J., Ibigbam, T.B. and Odeja, O., Effect of Chitosan Powder Prepared from Snail Shells to Remove Lead (II) Ion and Nickel (II) Ion from Aqueous Solution and Its Adsorption Isotherm Model. *American Journal of Applied Chemistry*, 4(4), 146-156, 2016.

[35] Zhang, L., Zeng, Y. and Cheng, C., Removal of Heavy Metal ions using Chitosan and Modified Chitosan: A Review. *Journal of Molecular Liquids*, 214, 175-191, 2016.

[36] Jeon, C. and Holl, W.H., Chemical Modification of Chitosan and Equilibrium Study for Mercury Ion Removal. *Water Research*, 37, 4770 – 4780, 2003.

[37] Benavent, M., Moreno, L. and Martinez, J., Sorption of Heavy Metals from Gold mining Wastewater using Chitosan. *Journal of the Taiwan Institute of Chemical Engineers*, 42, 976-988, 2011.

[38] Ngah, W.W., Teon, L.C. and Hanafiah, M.A.K.M., Adsorption of Dyes and Heavy Metal Ions by Chitosan Composites: A Review. *Carbohydrate Polymer*s, 83, 1446–1456, 2011.

[39] Ahmadi, M., Rahmani, H., Ramavand, B. and Kakavandi, B., Removal of Nitrate from Aqueous Solution using Activated Carbon Modified with Fenton reagents. *Desalination and Water Treatment*, 76, 265–275, 2017.